Korean J Physiol Pharmacol 2021;25(1):87-94
https://doi.org/10.4196/kjpp.2021.25.1.87

KJPP

Original Article

Nootkatol prevents ultraviolet radiation-induced photoaging *via* ORAI1 and TRPV1 inhibition in melanocytes and keratinocytes

Joo Han Woo[1,2], Da Yeong Nam[3], Hyun Jong Kim[4], Phan Thi Lam Hong[1,2], Woo Kyung Kim[2,4,*], and Joo Hyun Nam[1,2,*]

[1]Department of Physiology, Dongguk University College of Medicine, Gyeongju 38066, [2]Channelopathy Research Center (CRC), Dongguk University College of Medicine, Goyang 10326, [3]Avixgen, Seoul 06649, [4]Department of Internal Medicine, Graduate School of Medicine, Dongguk University, Goyang 10326, Korea

ARTICLE INFO

Received November 13, 2020
Revised December 6, 2020
Accepted December 6, 2020

***Correspondence**
Woo Kyung Kim
E-mail: wk2kim@naver.com
Joo Hyun Nam
E-mail: jhnam@dongguk.ac.kr

Key Words
Ion channel
Nootkatol
ORAI1 protein
Skin aging

ABSTRACT Skin photoaging occurs due to chronic exposure to solar ultraviolet radiation (UV), the main factor contributing to extrinsic skin aging. Clinical signs of photoaging include the formation of deep, coarse skin wrinkles and hyperpigmentation. Although melanogenesis and skin wrinkling occur in different skin cells and have different underlying mechanisms, their initiation involves intracellular calcium signaling via calcium ion channels. The ORAI1 channel initiates melanogenesis in melanocytes, and the TRPV1 channel initiates MMP-1 production in keratinocytes in response to UV stimulation. We aimed to develop a drug that may simultaneously inhibit ORAI1 and TRPV1 activity to help prevent photoaging. We synthesized nootkatol, a chemical derivative of valencene. TRPV1 and ORAI1 activities were measured using the whole-cell patch-clamp technique. Intracellular calcium concentration $[Ca^{2+}]_i$ was measured using calcium-sensitive fluorescent dye (Fura-2 AM). UV-induced melanin formation and MMP-1 production were quantified in B16F10 melanoma cells and HaCaT cells, respectively. Our results indicate that nootkatol (90 μM) reduced TRPV1 current by 94% ± 2% at –60 mV and ORAI1 current by 97% ± 1% at –120 mV. Intracellular calcium signaling was significantly inhibited by nootkatol in response to ORAI1 activation in human primary melanocytes (51.6% ± 0.98% at 100 μM). Additionally, UV-induced melanin synthesis was reduced by 76.38% ± 5.90% in B16F10 melanoma cells, and UV-induced MMP-1 production was reduced by 59.33% ± 1.49% in HaCaT cells. In conclusion, nootkatol inhibits both TRPV1 and ORAI1 to prevent photoaging, and targeting ion channels may be a promising strategy for preventing photoaging.

INTRODUCTION

Skin aging has become a critical factor as an indicator of beauty and of health [1,2]. Skin aging involves complex biological processes that are affected by intrinsic factors resulting from individual genetic backgrounds, as well as by extrinsic factors [3-5]. Among the various extrinsic factors that accelerate skin aging, ultraviolet (UV) irradiation due to sun exposure accounts for 80% of facial aging, and is referred to as photoaging [6]. Several anti-aging strategies have been developed, such as the use of moisturizing preparations, botulinum toxin, antioxidants, and photoprotection, for the prevention of photoaging [2,7]. However, none of these treatments has been effective. In this context, identifying mechanisms for the prevention of photoaging is of major interest in the dermatology and cosmetics industries, and research is being actively carried out globally.

Photoaging due to chronic UV irradiation is characterized by deep, coarse wrinkling, resulting from collagen degradation and irregular pigmentation [8,9]. Photoaging simultaneously causes wrinkle formation and skin pigmentation. However, the associated mechanisms occur independently via keratinocytes and melanocytes. According to previous studies, UV-mediated wrinkling

Author contributions: Conception and design of study: J.H.N., W.K.K. Conducting experiments, acquisition of data, analysis and interpretation of data: J.H.W., P.T.L.H., D.Y.N., H.J.K. Drafting the manuscript: J.H.W., J.H.N. Revising the manuscript critically for important intellectual content: W.K.K. Final approval of the version to be submitted: J.H.N., W.K.K. All authors have read and approved the final manuscript.

is mainly caused by the secretion of collagen-degrading enzymes and matrix metalloproteinase-1 (MMP-1) by keratinocytes. Furthermore, pigmentation involves tyrosinase and tyrosinase-related proteins in melanocytes [10]. Research is therefore focused on inhibiting collagenase or elastase to block wrinkling, and on tyrosinase production to reduce pigmentation [11]. However, recent studies suggest that both MMP-1 production and melanogenesis involve intracellular Ca^{2+} signaling, which is mediated by calcium ion channels [6,10,12-18].

Store-operated Ca^{2+} entry (SOCE) is mediated by calcium release-activated calcium channel protein 1 (ORAI1) and endoplasmic reticulum (ER) Ca^{2+} sensor protein stromal interaction molecule 1 (STIM1), and is crucial for both melanogenesis and melanocyte proliferation [19-21]. UV irradiation can activate SOCE in melanocytes through direct and indirect pathways to modulate melanin synthesis and melanocyte proliferation. The importance of ORAI1 activity in melanogenesis has been previously identified by our group, as well as by other independent groups [15,17,19,20]. Intracellular Ca^{2+} regulation is also important for wrinkle formation. UV radiation mediates TRPV1 activation, which leads to an increase in intracellular Ca^{2+} concentration ($[Ca^{2+}]_i$) in keratinocytes [13,22,23]. This elevated $[Ca^{2+}]_i$ activates calcium-dependent protein kinase C and further promotes MMP-1 expression in human keratinocytes [23].

Therefore, drug candidates that can simultaneously modulate ORAI1 and TRPV1 may serve as a novel therapeutic strategy for potentially inhibiting collagen degradation and melanogenesis to protect against cutaneous photoaging [24,25]. In a recent study, we identified valencene as a chemical constituent of *Cyperus rotundus* rhizomes. Valencene from the hexane fraction effectively inhibits the activity of both TRPV1 and ORAI1, in addition to inhibiting UV-induced melanogenesis [18].

Based on previous research, we reaffirm that screening for molecules that can simultaneously inhibit TRPV1 and ORAI1 could be beneficial for identifying drug candidates that can alleviate photoaging. To identify new effective anti-photoaging compounds, we synthesized new compounds using the backbone of valencene. The anti-photoaging effects of the chemical derivatives of valencene were examined by screening for antagonistic effects on TRPV1 and ORAI1. We subsequently confirmed the inhibition of melanin synthesis and MMP-1 production by the compound nootkatol in response to UV irradiation.

METHODS

Preparation of valencene derivatives

Candidate valencene derivatives were selected by consideration of the structure-efficiency correlation of the derivatives. The presence of the two-ring structure, and any difference in efficacy based on the type and location of the functional group were considered. All chemicals except nootkatol were purchased from Sigma-Aldrich (St. Louis, MO, USA). We synthesized nootkatol directly using the method described in the Supplementary Materials and Methods.

Cell culture

HEK293T cell line was purchased from the ATCC (Manassas, VA, USA), and HaCaT and B16F10 cell lines were purchased from the Korean Cell Line Bank (Seoul, Korea). The cell lines were cultured in DMEM (Thermo Fisher Scientific, Waltham, MA, USA) supplemented with 10% heat-inactivated fetal bovine serum (WelGENE, Daegu, Korea), 100 U/ml penicillin, and 100 g/ml streptomycin (Thermo Fisher Scientific). The cells were incubated in a humidified CO_2 incubator containing 20% O_2 and 10% CO_2 at 37°C. The cells were subcultured at 60%–70% confluency, and the cell culture medium was replaced every 48–72 h. Normal human melanocytes (NHEMs; ATCC) were maintained in dermal cell basal medium (ATCC) and incubated under 5% CO_2 conditions at 37°C. The Melanocyte Growth Kit (ATCC) and phenol red (ATCC) were added as supplements. The cells were subcultured and moved to 25-cm^2 culture flasks (Thermo Fisher Scientific) one day prior to the patch-clamp experiment.

Transfection of hORAI1 and STIM1

cDNAs encoding human ORAI1 (hORAI1) and human STIM1 (hSTIM1) were purchased from Origene Technologies (Rockville, MD, USA). The cDNA was subcloned into the pcDNA3.1 vector (Thermo Fisher Scientific). Plasmid DNA encoding human TRPV1 (hTRPV1, pcDNA5/FRT) was provided by Prof. Sung Joon Kim (Seoul National University, Seoul, Korea). The HEK293T cells were transfected with TurboFect transfection reagent (Thermo Fisher Scientific), and approximately 0.1×10^6 cells were plated on a culture plate 24 h before transfection. Measurements were performed 24 h after transfection.

Electrophysiology

hTRPV1 (I_{TRPV1}) and ORAI1 (I_{ORAI1}) currents were evaluated through conventional whole-cell recordings in voltage-clamp mode using a patch-clamp (Molecular Devices, San Jose, CA, USA) [15,16]. The cells were transferred into a perfusion bath chamber (Warner Instruments, Hamden, CT, USA) mounted on the stage of an inverted microscope (Nikon, Tokyo, Japan). The perfusion rate of the bath solution was 3 ml/min. A patch-clamp amplifier (Axopatch 700B), Digidata 1440A (Molecular Devices, Sunnyvale, CA, USA), and pCLAMP software v10.4 were used to acquire data and apply command pulses. The recorded current data were sampled at 10 kHz and lowpass filtered at 5 kHz. The recorded voltage and current data were analyzed using Clampfit 10.4 (Molecular Devices), Origin 8.0 (MicroCal, Northampton,

MA, USA), and Prism 6.0 (GraphPad, Inc., La Jolla, CA, USA). A horizontal flaming brown micropipette puller (model P97) was used to produce patch pipettes with thin-walled borosilicate glass (World Precision Instruments, Sarasota, FL, USA). Patch pipettes with a free-tip resistance of 2–3 MΩ were used to facilitate gigaseal formation.

To measure I_{TRPV1}, 1 μM capsaicin was used to activate I_{TRPV1}. To determine the basal current, 1 μM N-(4-tert-Butylphenyl)-4-(3-chloropyridin-2-yl)piperazine-1-carboxamide (BCTC), a potent TRPV1 antagonist, was added to the external solution at the end of the experiment. Every 20 sec, voltage ramp protocols (–100 to 100 mV, –10 mV holding potential, 100 msec) were applied to record I_{TRPV1}. To measure I_{ORAI1}, the STIM1 protein must be present in the ER membrane. Therefore, we co-transfected HEK293T cells with hSTIM1 and hORAI1. To deplete ER Ca^{2+} stores via inositol 1,4,5-trisphosphate (IP_3) receptor activation, 20 μM IP_3 was included in the internal pipette solution. IP_3-mediated depletion of ER Ca^{2+} stores can activate SOCE, referred to as ORAI1 currents. The holding potential was –10 mV, with voltage ramp-like pulses (–130 to +70 mV) over 100 msec for every 30 sec of recording, to measure the current–voltage relationship (I–V curves). Under these conditions, inwardly rectifying current (I_{ORAI1}) was consistently observed, with a reversal potential of approximately +50 mV. We therefore determined that I_{ORAI1} was generated by ORAI1 channels. Electrophysiological recordings were documented based on conventional whole-cell patch-clamp recordings.

Individual solutions were used to measure I_{TRPV1} and I_{Orai1}. For I_{TRPV1}, the internal solution contained CsCl (140 mM), NaCl (10 mM), ethylene glycol tetraacetic acid (EGTA, 5 mM), MgATP (3 mM), and 4(2hydroxyethyl)1piperazine ethanesulfonic acid (HEPES, 10 mM) at a pH of 7.2 (titrated with CsOH). The external solution contained NaCl (140 mM), KCl (4 mM), $MgCl_2$ (1 mM), EGTA (1 mM), Dglucose (5 mM), and HEPES (10 mM) at pH 7.4 (titrated with NaOH). After confirming the basal current, capsaicin-evoked activity was induced by adding capsaicin (1 μM) to the external solution. The IP_3-containing pipette solution was placed on an ice block.

Tyrosinase assay

Mushroom tyrosinase inhibitory activity was measured by following a previously reported method with modifications [26]. Briefly, a mixture containing 0.2 ml of the sample dissolved in DMSO, 1.0 ml of levodopa (1.5 mM), and 1.8 ml of sodium phosphate buffer (0.07 M, pH 6.8) was added to 0.1 ml of enzyme solution (1,000 U/ml), followed by incubation for 10 min at 30°C. The enzymes were inactivated using an ice bath, and enzyme activity was measured at 475 nm. The final concentration of kojic acid and nootkatol was adjusted to 200 μM.

3-(4,5-dimethylthiazol-2-yl)-2,5-diphenyltetrazolium bromide (MTT) cell viability assay

The cytotoxicity of nootkatol was tested by performing an MTT assay (Sigma-Aldrich), following the manufacturer's instructions. In brief, 2.5×10^4 cells were transferred to 24-well culture plates 24 h before the experiment. After overnight incubation at 37°C, keratinocytes (HaCaT cells) and melanocytes (B16F10 cells) were treated with various concentrations of nootkatol. After treating cells with nootkatol for 24 h, MTT (Sigma-Aldrich) was added to the plates, followed by incubation for 4 h. To dissolve the formazan crystals, the medium was removed, and 100 μl of DMSO was added at the end of incubation, following which the plates were incubated at 25°C for 30 min. The optical density of the cells was investigated using a plate reader (Powerwave x; Bio-Tek Instruments Inc., Winooski, VT, USA) at 540 nm.

MMP-1 assay

HaCaT cells were seeded at a density of 0.1×10^6/ml in 24-well plates and incubated for 24 h at 37°C. After exposure to UVB (16 mJ/cm^2), the cells were treated with 7.5 μg/ml nootkatol. The samples were maintained at 37°C for an additional 24 h. The supernatant was collected after centrifugation (1,000 *g*, 20 min), and the total amount of MMP-1 in the supernatant was determined using commercial ELISA kits for MMP-1 (ab100603; Abcam, Cambridge, MA, USA) following the manufacturer's protocol.

Measuring $[Ca^{2+}]_i$ using Fura-2

Fura-2 acetoxymethyl ester (Fura-2 AM; Thermo Fisher Scientific), a Ca^{2+} fluorescent indicator, was used to measure $[Ca^{2+}]_i$. Fura-2 AM (2 μM) was added to NHEMs in normal tyrode (NT) solution. The cells with Fura-2 AM were incubated for 45 min and washed twice with NT at 37°C. NT solution was composed of NaCl (145 mM), HEPES (10 mM), glucose (5 mM), KCl (3.6 mM), $CaCl_2$ (2 mM), and $MgCl_2$ (1 mM) at pH 7.4. Fluorescence measurements were made with an inverted microscope (Nikon Eclipse Ti; Nikon, Osaka, Japan) with a camera (sCMOS pco.edge 4.2; PCO, Kelheim, Germany) and an illuminator (pE-340 fura; CoolLED, Andover, UK). Samples were exposed to excitation wavelengths of 380 nm for 30 msec and 340 nm for 100 msec, and the data were recorded at an emission wavelength of 510 nm. Image analysis was performed using NIS-Element AR Version 5.00.00 (Nikon).

Statistical analysis

All data are presented as mean ± standard error of the mean. Statistical differences were analyzed by one-way analysis of variance (ANOVA, Bonferroni's *post-hoc*). P-values less than 0.05 were regarded as statistically significant. In the table, *, **, and

*** indicate $p < 0.05$, 0.01, and 0.001, respectively. Prism 6.0 and Origin 8.0 software were used for the statistical analyses. The number of tests (N values) are indicated for each experiment.

RESULTS

Screening valencene derivatives

The inhibitory effects of valencene on both hORAI1 and hTRPV1 channels, with less potent effect on hTRPV1 was demonstrated by our previous study [18]. Furthermore, valencene had potent inhibitory effects on UV-induced melanogenesis without directly inhibiting tyrosinase [18]. To identify compounds that can act more effectively on hTRPV1, we investigated the action of the four valencene derivatives: nootkatol, nootkatone, decaline, and valencene-13-aldehyde (Supplementary Fig. 1). Screening was performed using the whole-cell patch-clamp method at a derivative concentration of 90 μM. Nootkatol showed potent inhibitory effects on both I_{ORAI1} and I_{TRPV1} (Table 1).

Table 1. Effects of valencene derivatives on I_{TRPV1} and I_{ORAI1} at 90 μM

Compound	$(I/I_{con} \times 100\%) \pm$ SEM (n)	
	I_{TRPV1} at –60 mV	I_{ORAI1} at –120 mV
Control[a]	100	100
Valencene (Nam *et al*. [18], 2016)	31.2 ± 15.73 (3)	5.58 ± 2.12 (4)
Nootkatol	6.3 ± 2.36 (7)	3.4 ± 1.43 (4)
Nootkatone	176.2 ± 18.01 (3)	53.4 ± 7.86 (5)
Valencene-13-aldehyde	53.9 ± 9.59 (4)	57.1 ± 7.78 (6)
Decaline	139.5 ± 11.07 (4)	87.5 ± 5.71 (5)

Values in parentheses are the total number (n) of experiments at each concentration. Data represent remaining current compared to control, normalized to 100%, and are presented as the mean ± standard error of the mean (SEM). [a]Control indicates the normalized value at the steady-state peak current before treatment with compounds.

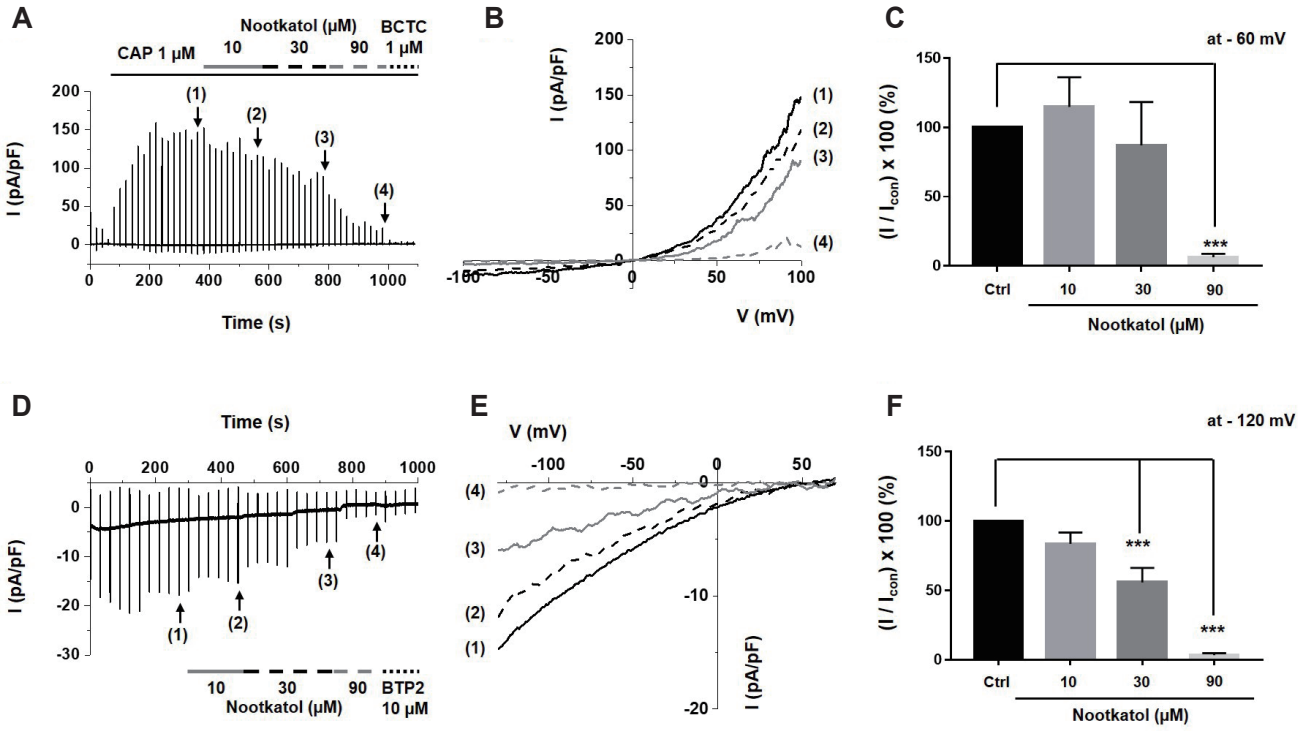

Fig. 1. Inhibitory effects of nootkatol on the human TRPV1 (hTRPV1) and human ORAI1 (hORAI1) currents. (A) Representative chart trace recording of hTRPV1 inhibited by nootkatol in hTRPV1-overexpressing HEK293T cells. The solid line indicates the holding current, whereas solid bars indicate the corresponding current induced by ramp-like pulse. After hTRPV1 activation by 1 μM capsaicin, the marked states indicate the steady-state currents of each condition, namely control (1) and treatment with 10 (2), 30 (3), and 90 μM (4) nootkatol. (B) Related current-voltage (I–V) relationship curve at the steady-state of the control (1) and cells treated with 10 (2), 30 (3), and 90 μM (4) nootkatol. (C) Summary of current inhibition by nootkatol treatment. Current amplitude is normalized to control current at –60 mV (mean ± standard error of the mean [SEM], n = 7, 4, 4, 7, respectively) (***$p < 0.001$). (D) Representative chart trace recording of hORAI1 inhibited by nootkatol in hORAI1-overexpressing HEK293T cells. (E) Related current-voltage (I–V) relationship curve at the steady-state of the control (1) and cells treated with 10 (2), 30 (3), and 90 μM (4) nootkatol. (F) Summary of the current level of hORAI1 upon nootkatol treatment. Current amplitude is normalized to control current at –120 mV (mean ± SEM, n = 7, 6, 6, 4, respectively) (***$p < 0.001$).

 https://doi.org/10.4196/kjpp.2021.25.1.87

Inhibitory effects of nootkatol on I_{TRPV1}

To identify the detailed inhibitory effects of nootkatol on I_{TRPV1} related to MMP-1 expression, various concentrations of nootkatol were added to an external solution, and the rates of I_{TRPV1} inhibition were compared. Fig. 1A indicates a representative trace of I_{TRPV1} and its inhibition by nootkatol. The associated I–V curves at the peak I_{TRPV1} (1) and upon treatment with 10 (2), 30 (3), and 90 μM (4) nootkatol were prepared using a ramp-like pulse protocol (–100 to 100 mV) (Fig. 1B). To analyze the antagonistic effects of nootkatol, the currents were obtained at a clamp voltage of –60 mV and presented as normalized amplitudes (I/I_{con} ×100%) (Fig. 1C). The normalized amplitudes of I_{TRPV1} were 115% ± 21%, 87% ± 31%, and 6% ± 2% at nootkatol concentrations of 10, 30, and 90 μM, respectively.

Inhibitory effects of nootkatol on I_{ORAI1}

As previously discussed, I_{ORAI1} is important for UV-induced melanogenesis. After checking the steady state of I_{ORAI1}, 10, 30, and 90 μM nootkatol were sequentially applied to the external solution, as in the I_{TRPV1} experiments (Fig. 1D, E). Normalized amplitudes of I_{ORAI1} were reduced to 84% ± 8%, 56% ± 11%, and 3% ± 1% upon nootkatol treatment at –120 mV (Fig. 1F).

Inhibition of intracellular Ca^{2+} signaling by nootkatol

Increased $[Ca^{2+}]_i$ due to Ca^{2+} channel activation initiates various biochemical processes involving melanogenesis and MMP-1 expression. We confirmed whether nootkatol could inhibit $[Ca^{2+}]_i$. In human primary melanocytes, SOCE modulated the increase in $[Ca^{2+}]_i$ *via* ER store depletion. Thapsigargin is a specific inhibitor of sarcoplasmic/endoplasmic reticulum Ca^{2+}-ATPase (SERCA), which can deplete ER Ca^{2+} stores in the absence of extracellular Ca^{2+}. We added 2 mM Ca^{2+} to thapsigargin to determine whether the Ca^{2+} influx was enhanced by prior Ca^{2+} store depletion. As shown in Fig. 2A, adding 2 mM Ca^{2+} clearly activated SOCE, and treatment with nootkatol (10 and 100 μM) inhibited $[Ca^{2+}]_i$ by

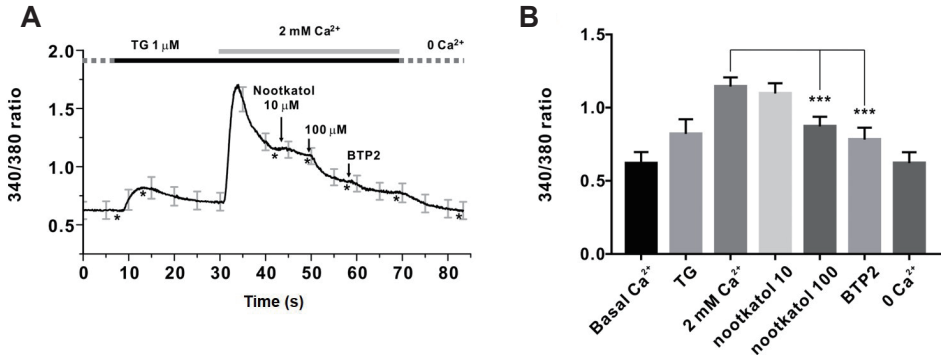

Fig. 2. Inhibition of thapsigargin-induced store-operated Ca^{2+} entry (SOCE) by nootkatol in primary human melanocytes. (A) Representative trace for intracellular Ca^{2+} measurement by Fura-2 in primary human melanocytes. Treatment with 10 and 100 μM nootkatol after the 2 mM Ca^{2+} add-back procedure partially inhibited $[Ca^{2+}]_i$. To confirm the basal $[Ca^{2+}]_i$, 10 μM BTP2, a potent ORAI1 inhibitor, was used. Asterisks (*) indicate the "time point" for each chemical treatment. (B) Summary of the inhibitory effects of 10 and 100 μM nootkatol and 10 μM BTP2 on $[Ca^{2+}]_i$ in primary human melanocytes. ***p < 0.001 *vs.* the control (mean ± standard error of the mean, n = 8).

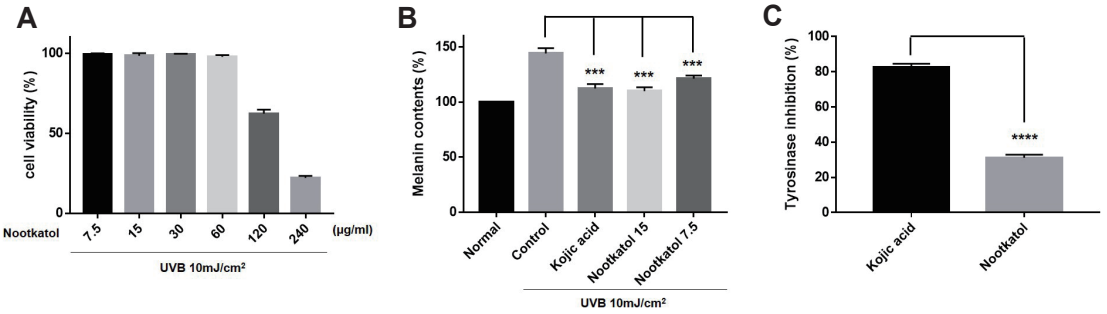

Fig. 3. Inhibitory effect of nootkatol on ultraviolet radiation (UV)-induced melanogenesis. (A) In the cytotoxicity assay performed with B16F10 cells, nootkatol-treated cells showed 99.22% ± 0.70%, 98.36% ± 1.65%, 99.20% ± 0.52%, 97.80% ± 1.07%, 62.29% ± 2.45%, and 22.06% ± 1.26% cell survival rate at 7.5, 15, 30, 60, 120, and 200 μg/ml, respectively (mean ± standard error of the mean [SEM], n = 3). (B) The inhibitory effect on UV-induced melanogenesis in B16F10 cells was 84.14% ± 1.54% and 76.38% ± 5.90% at 7.5 μg/ml and 15 μg/ml nootkatol, respectively. Kojic acid showed 78.12% ± 7.29% melanin inhibition at 15 μg/ml (mean ± SEM, n = 3) (***p < 0.001). (C) Direct tyrosinase inhibitory activity of 200 μM nootkatol and kojic acid (positive control) (mean ± SEM, n = 3) (****p < 0.0001).

6.9% ± 5.72% and 51.6% ± 0.98%, respectively (Fig. 2B).

Inhibitory effects of nootkatol on UV-induced melanogenesis in B16F10 cells

To identify the anti-UV-induced melanogenesis activity of nootkatol, the UV-induced melanin contents were measured in B16F10 mouse melanoma cells. Before the melanogenesis test, the cytotoxicity of nootkatol in B16F10 cells was determined. The results indicate that nootkatol did not exert harmful effects on cell viability at concentrations < 60 μg/ml (Fig. 3A).

The cells were then pretreated with 7.5 (≈ 35 μM) or 15 μg/ml (≈ 70 μM) nootkatol prior to 10 mJ/cm^2 UV exposure. Melanin levels were measured after 48 h of UV exposure, and the melanin content (144.21% ± 4.80%) that increased upon UV irradiation was dose-dependently decreased to 121.27% ± 2.75% and 109.89% ± 3.46% upon treatment with 7.5 and 15 μg/ml nootkatol, respectively. At a concentration of 15 μg/ml (≈ 105 μM), kojic acid also decreased the melanin content (112.31% ± 4.04%) (Fig. 3B). Therefore, nootkatol treatment can decrease UV radiation-induced melanin production.

To confirm whether nootkatol directly affects tyrosinase activity, a mushroom tyrosinase activity assay was performed. As shown in Fig. 4, even at 200 μM, nootkatol treatment showed only a slight inhibitory effect on tyrosinase (31.3% ± 1.75% inhibition). This is in contrast to the effects of 200 μM kojic acid on tyrosinase (82.6% ± 1.96% inhibition), which directly inhibits tyrosinase (Fig. 3C). These results suggest that the inhibition of UV-induced melanogenesis by nootkatol is mainly due to the inhibition of intracellular calcium signaling, and is not caused by a direct effect on tyrosinase.

MMP-1 production in response to UV irradiation was reduced by nootkatol in HaCaT cells

We investigated the protective effect of nootkatol against UV irradiation-mediated MMP-1 production in HaCaT cells. The cytotoxicity of nootkatol was screened by the MTT assay in HaCaT cells. As indicated in Fig. 4A, 15 μg/ml nootkatol exhibited low cytotoxicity in HaCaT cells. The level of secreted MMP-1 was measured in the culture media 48 h after UV irradiation. Pretreatment of HaCaT cells with 7.5 μg/ml nootkatol before 16 mJ/cm^2 UV exposure, significantly reduced MMP-1 activity (59.33% ± 1.49%) compared to that in the UV exposed cells (Fig. 4B).

DISCUSSION

Intracellular calcium signaling is a key biological process involved in UV-induced photoaging, including skin pigmentation and wrinkle formation [2,7]. Many types of calcium ion channels are expressed in keratinocytes and melanocytes [21,27-29]; however, we selected TRPV1 and ORAI1 for this investigation.

During UV-induced wrinkle formation, increased $[Ca^{2+}]_i$ due to TRPV1 activation induces gasdermin-C gene expression. Gasdermin-C expression is mediated by the cytoplasmic 1 (NFATc1) pathway, wherein NFATc1 corresponds to the Ca^{2+}/calcineurin/nuclear factor of activated T cells [14]. Upregulated gasdermin-C expression increases the production of MMP-1, which dose-dependently degrades collagen and elastin fibers that maintain skin elasticity and block laxity [13,14]. Moreover, it was reported that UV irradiation could also increase TRPV1 expression [22]. This suggests that repeated UV irradiation can worsen skin wrinkling via TRPV1 [23].

UV-induced melanogenesis occurs via direct and indirect pathways. The indirect pathway is the most well-known mechanism of melanogenesis. UV stimulation activates keratinocytes, and the keratinocytes secrete various keratinocyte-derived factors. These include α-melanocyte-stimulating hormone (α-MSH), adrenocorticotropic hormone (ACTH), and endothelin-1 (ET-1) [30,31]. These factors affect the neighboring melanocytes via specific receptors. Changing $[Ca^{2+}]_i$ due to receptor activation is an

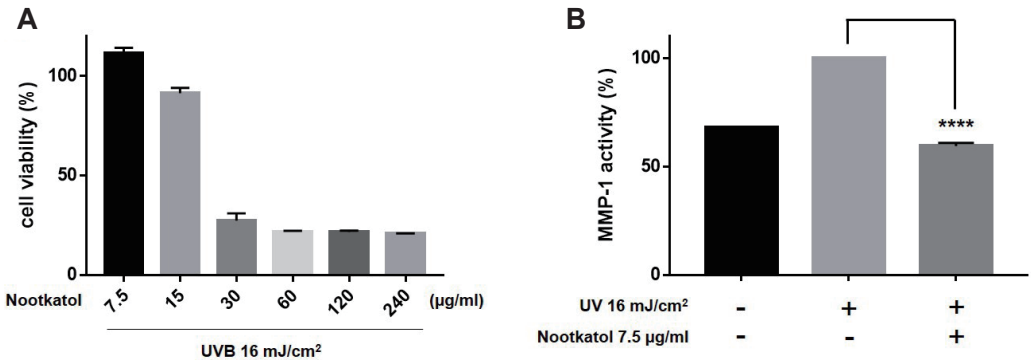

Fig. 4. Effects of nootkatol on ultraviolet radiation (UV)-induced matrix metalloproteinase-1 (MMP-1) production. (A) Treatment with 7.5, 15, 30, 60, 120, and 240 μg/ml nootkatol showed 111.37% ± 2.88%, 91.33% ± 2.74%, 27.24% ± 3.73%, 21.59% ± 0.51%, 21.50% ± 0.75%, and 20.65% ± 0.23% cell viability, respectively (n = 3). (B) MMP-1 level, expressed as % of control, following exposure to UVB irradiation (16 mJ/cm^2) alone and with nootkatol pretreatment (7.5 μg/ml, 59.33% ± 1.49%) (mean ± standard error of the mean, n = 3) (****p < 0.0001).

important cue for melanin synthesis, which is usually mediated by ER Ca^{2+} stores and calcium ion channels [32]. It was recently reported that ORAI1-STIM1 complex formation due to α-MSH stimulation is important for both intracellular calcium signaling and adenylyl cyclase 6 (ADCY6) activation. This molecule directly interacts with STIM1 via a membrane-delimited pathway, controlling melanocyte proliferation and melanin synthesis [20]. In the direct pathway, direct UV stimulation can increase intracellular calcium signaling, which is governed by rhodopsin via a G protein- and phospholipase C-mediated pathway [33]. Our previous studies have revealed that ORAI1 contributes to the generation of calcium signaling in response to direct UV irradiation of melanocytes [15,17]. Another group has suggested TRPA1 as a candidate for generating calcium signaling in human melanocytes via UV irradiation [34].

A previous study demonstrated that valencene from the rhizomes of *C. rotundus* inhibits TRPV1 and ORAI1, thereby effectively suppressing UV-induced melanogenesis [16]. However, valencene inhibited TRPV1 less potently than it inhibited ORAI1.

Our current study aimed to identify chemical candidates that can simultaneously inhibit TRPV1 and ORAI1, and to determine the potential of these chemicals to inhibit melanogenesis and MMP-1 production, which are the typical phenomena during photoaging. Several compounds (Supplementary Fig. 1) based on the chemical structure of valencene were selected to develop more effective anti-photoaging substances that show an inhibitory effect on both TRPV1 and ORAI1. By screening using the whole-cell patch-clamp method, we discovered that nootkatol could potently inhibit TRPV1 and ORAI1 channels (Fig. 1). To confirm its suppressive effects on UV-induced melanogenesis and MMP-1 production, melanin synthesis and MMP-1 production were examined in B16F10 and HaCaT cells, respectively. The results revealed that the melanin content elevated in response to UV irradiation was significantly decreased by nootkatol treatment via suppression of $[Ca^{2+}]_i$. However, high concentrations of nootkatol did not affect the direct inhibition of tyrosinase considerably (Figs. 2 and 3). Pretreatment with nootkatol also decreased MMP-1 production by UV irradiation (16 mJ/cm^2) compared to the control (Fig. 4). Our findings imply that nootkatol treatment may be effective in preventing UV-induced photoaging.

In conclusion, our data demonstrate the potential effectiveness of our strategy for screening for anti-photoaging agents targeting TRPV1 and ORAI1. Our synthesized chemical, nootkatol, evidently reduced both UV-induced MMP-1 production and melanogenesis by inhibiting TRPV1 and ORAI1 in keratinocytes and melanocytes, respectively. However, the inhibitory effects of nootkatol on melanogenesis and MMP-1 could not be investigated in detail, and needs to be further elucidated in future studies.

ACKNOWLEDGEMENTS

This research was supported by the Basic Science Research Program through the National Research Foundation of Korea (NRF) funded by the Ministry of Education of South Korea (No. NRF-2019R1I1A3A01041391).

CONFLICTS OF INTEREST

The authors declare no conflicts of interest.

SUPPLEMENTARY MATERIALS

Supplementary data including one figure can be found with this article online at https://doi.org/10.4196/kjpp.2021.25.1.87.

REFERENCES

1. Gupta MA, Gilchrest BA. Psychosocial aspects of aging skin. *Dermatol Clin*. 2005;23:643-648.
2. Shanbhag S, Nayak A, Narayan R, Nayak UY. Anti-aging and sunscreens: paradigm shift in cosmetics. *Adv Pharm Bull*. 2019;9:348-359.
3. Dobos G, Lichterfeld A, Blume-Peytavi U, Kottner J. Evaluation of skin ageing: a systematic review of clinical scales. *Br J Dermatol*. 2015;172:1249-1261.
4. Farage MA, Miller KW, Elsner P, Maibach HI. Intrinsic and extrinsic factors in skin ageing: a review. *Int J Cosmet Sci*. 2008;30:87-95.
5. Kohl E, Steinbauer J, Landthaler M, Szeimies RM. Skin ageing. *J Eur Acad Dermatol Venereol*. 2011;25:873-884.
6. Amaro-Ortiz A, Yan B, D'Orazio JA. Ultraviolet radiation, aging and the skin: prevention of damage by topical cAMP manipulation. *Molecules*. 2014;19:6202-6219.
7. Rattanawiwatpong P, Wanitphakdeedecha R, Bumrungpert A, Maiprasert M. Anti-aging and brightening effects of a topical treatment containing vitamin C, vitamin E, and raspberry leaf cell culture extract: a split-face, randomized controlled trial. *J Cosmet Dermatol*. 2020;19:671-676.
8. Gilchrest BA. Photoaging. *J Invest Dermatol*. 2013;133(E1):E2-E6.
9. Krutmann J, Morita A, Chung JH. Sun exposure: what molecular photodermatology tells us about its good and bad sides. *J Invest Dermatol*. 2012;132(3 Pt 2):976-984.
10. Park HY, Kosmadaki M, Yaar M, Gilchrest BA. Cellular mechanisms regulating human melanogenesis. *Cell Mol Life Sci*. 2009;66:1493-1506.
11. Schieke SM. [Photoaging and infrared radiation. Novel aspects of molecular mechanisms]. *Hautarzt*. 2003;54:822-824. German.
12. Choi TY, Park SY, Jo JY, Kang G, Park JB, Kim JG, Hong SG, Kim CD, Lee JH, Yoon TJ. Endogenous expression of TRPV1 channel in cultured human melanocytes. *J Dermatol Sci*. 2009;56:128-130.
13. Kusumaningrum N, Lee DH, Yoon HS, Kim YK, Park CH, Chung JH. Gasdermin C is induced by ultraviolet light and contributes to MMP-1 expression via activation of ERK and JNK pathways. *J Der-*

matol Sci. 2018;90:180-189.
14. Kusumaningrum N, Lee DH, Yoon HS, Park CH, Chung JH. Ultraviolet light-induced gasdermin C expression is mediated via TRPV1/calcium/calcineurin/NFATc1 signaling. *Int J Mol Med*. 2018;42:2859-2866.
15. Lee DU, Weon KY, Nam DY, Nam JH, Kim WK. Skin protective effect of guava leaves against UV-induced melanogenesis via inhibition of ORAI1 channel and tyrosinase activity. *Exp Dermatol*. 2016;25:977-982.
16. Nam JH, Lee DU. Inhibitory effect of oleanolic acid from the rhizomes of Cyperus rotundus on transient receptor potential vanilloid 1 channel. *Planta Med*. 2015;81:20-25.
17. Nam JH, Lee DU. Foeniculum vulgare extract and its constituent, trans-anethole, inhibit UV-induced melanogenesis via ORAI1 channel inhibition. *J Dermatol Sci*. 2016;84:305-313.
18. Nam JH, Nam DY, Lee DU. Valencene from the rhizomes of Cyperus rotundus inhibits skin photoaging-related ion channels and Uv-induced melanogenesis in B16F10 melanoma cells. *J Nat Prod*. 2016;79:1091-1096.
19. Motiani RK, Tanwar J, Raja DA, Vashisht A, Khanna S, Sharma S, Srivastava S, Sivasubbu S, Natarajan VT, Gokhale RS. STIM1 activation of adenylyl cyclase 6 connects Ca^{2+} and cAMP signaling during melanogenesis. *EMBO J*. 2018;37:e97597.
20. Stanisz H, Stark A, Kilch T, Schwarz EC, Müller CS, Peinelt C, Hoth M, Niemeyer BA, Vogt T, Bogeski I. ORAI1 Ca^{2+} channels control endothelin-1-induced mitogenesis and melanogenesis in primary human melanocytes. *J Invest Dermatol*. 2012;132:1443-1451.
21. Stanisz H, Vultur A, Herlyn M, Roesch A, Bogeski I. The role of Orai-STIM calcium channels in melanocytes and melanoma. *J Physiol*. 2016;594:2825-2835.
22. Lee YM, Kim YK, Chung JH. Increased expression of TRPV1 channel in intrinsically aged and photoaged human skin in vivo. *Exp Dermatol*. 2009;18:431-436.
23. Lee YM, Kang SM, Chung JH. The role of TRPV1 channel in aged human skin. *J Dermatol Sci*. 2012;65:81-85.
24. Jiang SJ, Chu AW, Lu ZF, Pan MH, Che DF, Zhou XJ. Ultraviolet B-induced alterations of the skin barrier and epidermal calcium gradient. *Exp Dermatol*. 2007;16:985-992.
25. Lee SE, Lee SH. Skin barrier and calcium. *Ann Dermatol*. 2018;30:265-275.
26. Tajima R, Oozeki H, Muraoka S, Tanaka S, Motegi Y, Nihei H, Yamada Y, Masuoka N, Nihei K. Synthesis and evaluation of bibenzyl glycosides as potent tyrosinase inhibitors. *Eur J Med Chem*. 2011;46:1374-1381.
27. Bellono NW, Oancea EV. Ion transport in pigmentation. *Arch Biochem Biophys*. 2014;563:35-41.
28. Caterina MJ, Pang Z. TRP channels in skin biology and pathophysiology. *Pharmaceuticals (Basel)*. 2016;9:77.
29. Elsholz F, Harteneck C, Muller W, Friedland K. Calcium--a central regulator of keratinocyte differentiation in health and disease. *Eur J Dermatol*. 2014;24:650-661.
30. Abdel-Malek ZA, Kadekaro AL, Swope VB. Stepping up melanocytes to the challenge of UV exposure. *Pigment Cell Melanoma Res*. 2010;23:171-186.
31. Lee AY. Recent progress in melasma pathogenesis. *Pigment Cell Melanoma Res*. 2015;28:648-660.
32. Schallreuter KU, Kothari S, Chavan B, Spencer JD. Regulation of melanogenesis--controversies and new concepts. *Exp Dermatol*. 2008;17:395-404.
33. Wicks NL, Chan JW, Najera JA, Ciriello JM, Oancea E. UVA phototransduction drives early melanin synthesis in human melanocytes. *Curr Biol*. 2011;21:1906-1911.
34. Bellono NW, Kammel LG, Zimmerman AL, Oancea E. UV light phototransduction activates transient receptor potential A1 ion channels in human melanocytes. *Proc Natl Acad Sci U S A*. 2013;110:2383-2388.